

## **Extracting hierarchical dynamical structure from a multistable geological system—the Himalayan paleomonsoon**

**Enter authors here: M. R. Gipp<sup>1</sup>**

<sup>1</sup>Marine Mining Corp, 856 Millwood Rd., Toronto, ON M4G 1W6 CANADA

Corresponding author: Michael Gipp ([drgipp@gmail.com](mailto:drgipp@gmail.com))

### **Key Points:**

- East Asian paleomonsoon proxy data suggest the monsoon system is multistable, with seven separate multistable “first-order states”
- The first-order states define four distinct modes of operation which have generally increased in complexity over the past 2.2 million years
- Hierarchy in the dynamics of the paleomonsoon system can be extracted from paleoclimatic records so that dynamic changes driven by insolation can be distinguished from those driven by tectonic activity.

## Abstract

The author presents an iterative approach to describing a data set, such as a paleoclimatic proxy or a model output, in terms of automata of successively higher order. The automata reflect dynamics acting on successively longer timescales and larger spatial scales. The method uses the computed probability density function from reconstructed state space portraits, over successive overlapping windows in time, of the record of magnetic susceptibility of loess and paleosols at Luochuan, central China. Areas of consistently high probability across several time windows represent areas of quasistability, which are used as the predictive and successor states of a succession of Markov Chains that characterize the variability of the strength of the East Asian paleomonsoon at different time scales. Seven metastable states are thus identified, forming four Markov Chains, which show a marked increase in complexity of behavior of the paleomonsoon system throughout the Quaternary. A higher-order automaton is suggested by the sequence of Markov Chains, suggesting differing cycles of dynamic behaviour in the Early and Late Quaternary.

## 1 Introduction

There are two sources of energy that drive changes at the earth's surface – heat energy from nuclear decay within the Earth, and heat energy produced by nuclear fusion within the Sun. The result at the earth's surface has been long cycles of tectonic changes and shorter cycles of climatic changes. The duality of energy sources allows for at least the possibility of hierarchical organization of geological processes, but reliably inferring such organization from observations remains a challenge.

There are numerous geological systems which may be investigated for hierarchical behaviour, but in order to investigate them, we require geological records which are long enough for the effects of tectonic processes on the system to have been preserved, and of sufficiently high resolution that climatic effects can be interpreted. Geological records from the East Asian paleomonsoon demonstrate that this system has persisted since at least the Late Neogene (Sun and Wang, 2005; Clift et al., 2008) and possibly the Late Eocene (Spicer et al., 2017) making this a prime target for investigating whether there is a hierarchy of dynamics that can be extracted. Paleogeography is known to influence the East Asian monsoon (Farnsworth *et al.*, 2019) due to the effects of the uplift of the Himalayan plateau on the hydrological system. The distribution of continental masses affects currents, especially poleward deflection of equatorial waters. Tectonics also exercises a large control on geochemical cycling across long timescales (Kleidon, 2012); the supercontinent cycle; the formation of continental crust (generally increasing through time); and CO<sub>2</sub> fluxes associated with uplift and weathering of mountain ranges (Menzies et al., 2018). Tectonics (particularly the supercontinent cycle) are on the highest level of the hierarchy, and are generally considered to set boundary conditions for most other earth processes.

Hierarchical organization is common in complex systems, including: biological systems (Alcocer-Cuarón et al., 2014); control over macroevolution (Okasha, 2012); and social systems and networks (Guimerà, et al., 2003; Mihn et al., 2010). Pattee (1972) observed that as a system develops more elaborate hierarchies, its behavior becomes simple (*i.e.*, emergence of global scale structure becomes more likely) as lower level entities become increasingly constrained in their

behavior, which tends to be far from equilibrium—an idea developed more thoroughly by Okasha (2012). Deep hierarchical structure, which indicates elaborate organization, leads to complex systems (e.g., Liu et al., 2014). This global behavior can be very complicated, and complex behaviour in a system may well be one of the fingerprints of hierarchical organization (Caraiani, 2013). Consequently, climatic effects which might otherwise be expected to disappear into chaos on larger scales instead develops highly ordered structure on a global spatial scale and on a timescale of tens to hundreds of thousands of years (Gipp, 2001). Such order is an “emergent property” of the system, and there is increasingly an understanding that emergence is tied to the hierarchical organization of networks of processes (Okasha, 2012; Kleidon, 2012). Emergent properties include multistability, which describes the coexistence of multiple stable states (also “equilibria” or “attractors”) within a system with a given set of forcings and boundary conditions (Feudel, 2008; Feudel et al., 2018); or as reorganizations of the system on a global scale, previously described as “innovation” (Crutchfield, 1994) or “irreversible change” (Nicolis, 1987).

Multistable phenomena are known to include biological and ecological systems (May, 1977); climate systems (Lucarini and Bodai, 2016); ice sheets (Robinson et al., 2012); neurological systems (Kelso, 2012); chemical oscillators (Crowley and Epstein, 1989); among many other types of natural and experimental systems (Feudel, et. al., 2018).

Examples of “innovation” in earth history may include the proposed change(s) in character of plate tectonics during the Archean; Neoproterozoic glaciations; mantle superplume events; and magnetic pole reversals. Recognizing innovation in Earth systems on the basis of geological time series is difficult due to our natural tendency to interpret new observations in terms of our current understanding (Crutchfield, 1994). Computational statistics can be used to provide insight by characterizing the complexity of Earth system behaviour in a manner that allows its hierarchical structure to be extracted. Innovation may then be reframed as reorganizations on different levels in the hierarchy of earth systems.

In this paper, the author extracts hierarchical information from the record of magnetic susceptibility of loess and paleosols at Luochuan, central China (Kukla et al., 1990), which covers the most significant portion of the Quaternary. The record, which displays multistability (Gipp, 2001), is first simplified by an approach which reduces the record to a series of Markov Chains, which are processed by statistical computational methods to extract hierarchical structure.

## 2 Methods

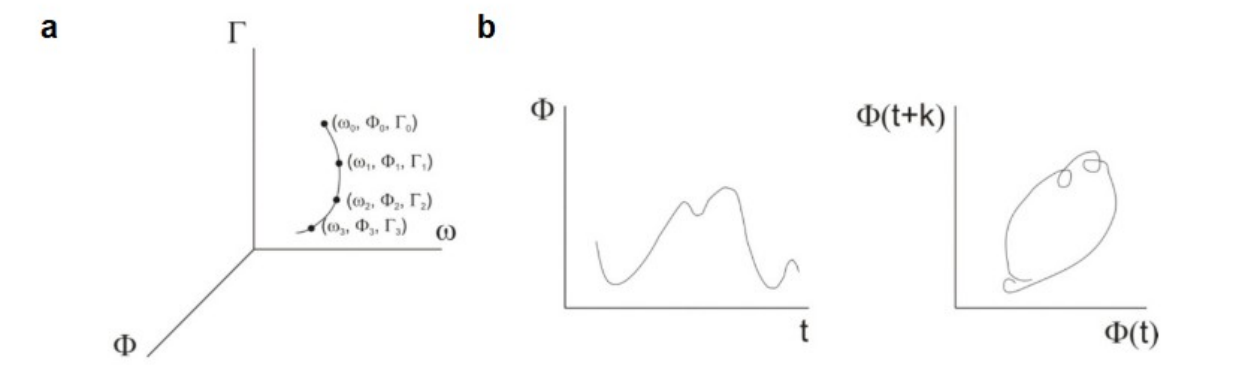
The method uses a technique introduced by Gipp (2001) involving reconstructing phase space portraits in two dimensions; contouring their probability density over successive windows in time to identify regions of phase space representing relatively stable behavior. These episodes of stable behavior are referred to hereafter as “first-order states”. Changes from one first-order state to another constitutes a bifurcation. Merrill (2010) proposed to use Markov Chains to describe observed bifurcations in a complex system – in the form of observational representations of transitional changes from one area of stability to another. Each possible transition is assigned a probability based on observed transitions. In this paper the probability of a transition is expressed as probability per unit of time ( $\text{ky}^{-1}$ ).

The sequence of first-order states defines an automaton (called a “second-order state” hereafter), which is a symbolic representation of the complexity of the system. The series of second-ordered

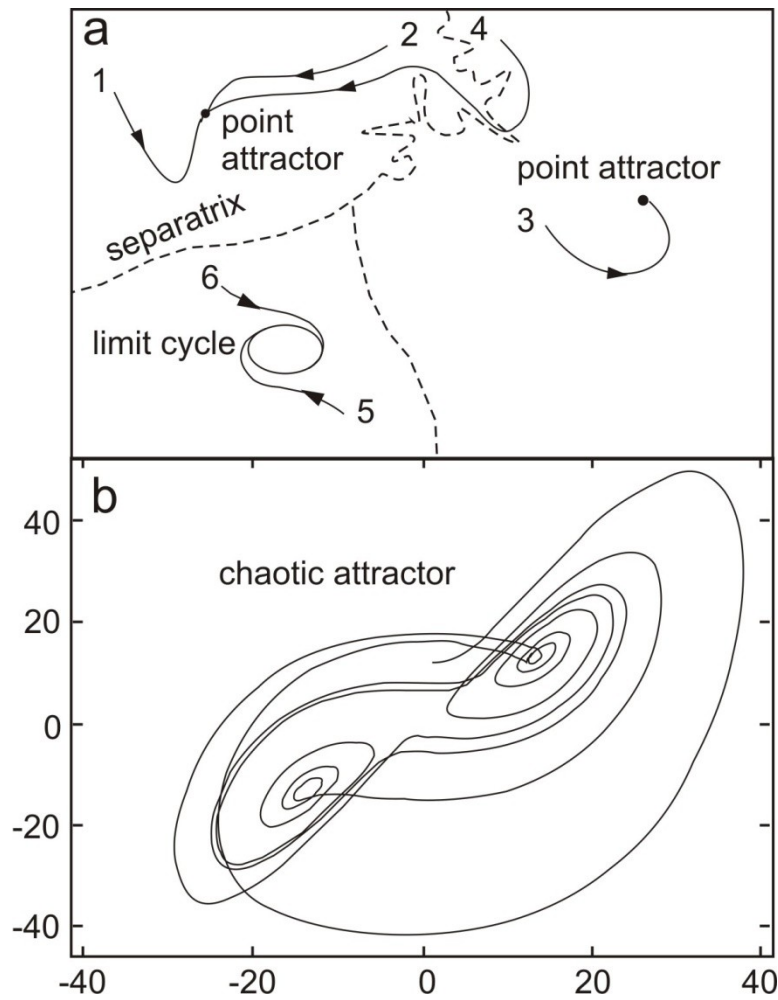
states can be described by another Markov Chain (a third-order state), which itself would be a single predictive or successor state to an automaton of yet higher dimension. Such analyses can be carried out in principle without limit to the level of complexity, but the limitations of the data do not allow the third- or higher-order states to be defined with confidence.

## 2.1 Flows and Phase space portraits

Reconstructed phase space portraits have been used to study the dynamics of complex time series for forty years (Packard et al., 1980; Abarbanel, 1996), including natural phenomena (Abarbanel and Lall, 1996; Gipp, 2001; Ghil et al., 2002). Such systems, were our knowledge about them perfect, would be described by a space of vectors defined by a minimum number of independent variables (figure 1). The vectors would allow us to determine how the system (represented at one moment of time by a single point in the space of vectors) will evolve through time. But our knowledge is imperfect, and we are unable to determine the true space of vectors. The reconstructed phase space portrait allows us to infer a space of vectors which is topologically equivalent to the ideal space (Han et al., 2019). Thus, the number of attractors will be the same, and there will be a one-to-one correspondence between the attractors or zones of attraction in our reconstructed state space and the ideal state space of the true vector space.

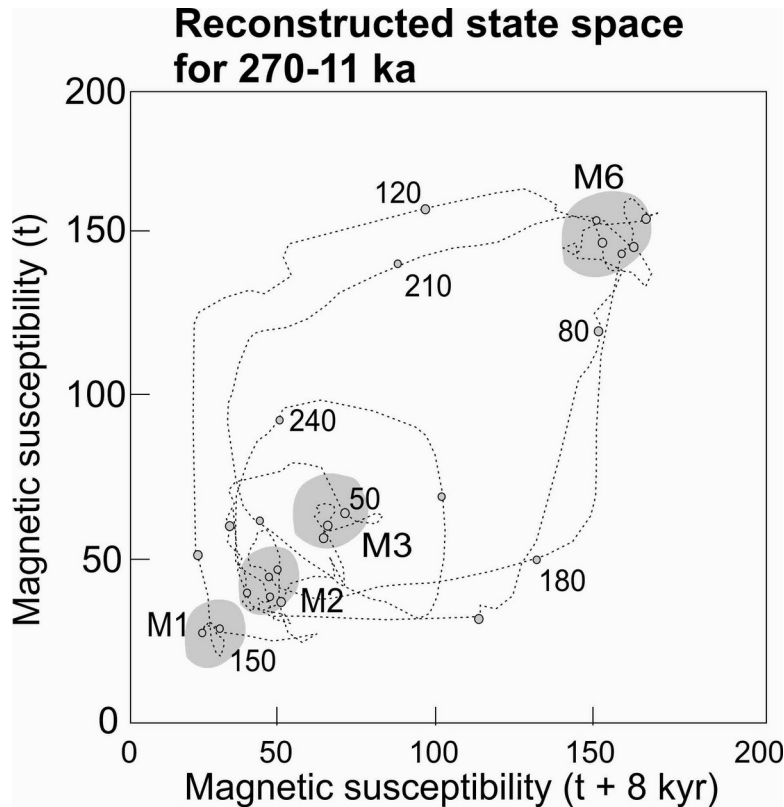


For continuous systems of differential equations, each state flows deterministically to a uniquely defined sequence of *successor states*, implying that two states which lie on different trajectories will remain so—hence, no line crossings occur (Hirsch and Smale, 1974). In purely chaotic systems, the future orbits of two arbitrarily close states will diverge at an exponential rate. In some systems, however, two states on different trajectories may evolve toward successor states which are arbitrarily close to one another. They may converge toward a single state which does not change in time. This unchanging state is called an *attractor*, and the behavior is described as *asymptotic stability* (figure 2a). Alternatively, they may not converge onto a particular point, but the successor states from any state within a small region of phase space may stay within a limited region of phase space. Such behavior is described as *Lyapunov stability* (Lyapunov, 1966). Other possible behaviors include “strange attractors” (figure 2b), and limit or “ghost” cycles (Ghil et al., 2002). Complex attractors are fractal in nature, and exhibit particular properties which make prediction of such a system very difficult. These dynamics are only apparent in the reconstructed phase space—they cannot be perceived in the one-dimensional plot of the time series.



Some dissipative systems with unstable dynamics generate multi-stable behavior (Anzo-Hernández et al., 2018), which there are different end states that are dependent on the initial conditions. There may be a number of disjoint Lyapunov-stable areas (LSA), each separated in phase space by a separatrix (Kauffman, 1993). At any given time, the state of the system occupies only one such LSA, so that their number therefore constitutes the total number of alternative long-term behaviors, or equilibrium states, of the system (Figure 2a). Since an LSA is likely to be smaller than the total allowable range of states, the system tends to become boxed into an LSA unless it is subjected to external forcing. When the state approaches a separatrix, small perturbations can trigger a change to a nearby state, which can result in chaotic changes in the evolution of the system (Feudel, 2008). Thus very complex behavior can arise in multistable systems.

Gipp (2001) used the probability density function (PDF) in the reconstructed phase space to identify LSAs in phase space. The probability density is computed from the amount of time the trajectory of the system lies within equally spaced overlapping bins divided by the length of the window, and the contours were drawn at 4.5 ky intervals (probability density 0.03). Areas of high probability density correspond to the central regions of basins of attraction. Regions of high probability density may result from multiple visits to the same region of phase space, or by a drop the rate of evolution of the system (*i.e.*, several consecutive states occupy the same general region of phase space). The relationship between the trajectory of the system through phase space and the interpreted LSAs from a PDF appear in figure 3.



## 2.2 Markov Chain Construction

The system's behavior can be characterized by the type, order, and number of attractors (or areas of stability) that are traced out as the system evolves through time. Areas of attraction are commonly described as 'states' (*e.g.*, 'glacial state' in Paillard, 2001) which can lead to confusion with the application of the same term in ergodic theory, in which 'state' represents an instantaneous position of the system in phase space (*i.e.*, a single observation). In order to reduce confusion, the author proposes the instantaneous position of the system be called a 'zero-order state' and each LSA will represent a 'first-order state'. Seven LSAs are observed, and they are designated M1 to M7.

The sequence of LSAs can be analyzed in a manner similar to a Markov process. The author wishes to note that the goal of this procedure is descriptive, even though the Markov Chain is used to describe purely stochastic processes dependent only on present conditions despite the author's work on long memory and the geological system displays long memory (Gipp, 2001). The method is used to characterize the time-evolution of the system as a sequence of transitions

from one predictive state to another, and the probability of transition from one first-order state to another. The definition of predictive states effects the transformation of the original numerical data into a series of symbols which permits the usage of symbolic dynamics (Strelief *et al.*, 2007).

Thus a sequence of LSAs may appear as a character string (*e.g.*, M1M4M2M1M3M4M5. . .). Higher order structure is obtained by representing this string by a Markov Chain, noting that in the above string, that M1 may be followed by M4 or M3, apparently with an even chance of either occurring; M2 is only followed by M1, M3 is only followed by M4, and M4 may be followed by M5 or M2. In the study below, probabilities of transitions are calculated from the number of a particular transition (*e.g.*, M1 to M3) divided by the total length of time that the predictive state is active. The character strings in the study are much longer than in the example above.

Second order states are identified by changes in the sequencing of the character strings. For instance, there are intervals as follows: M1M3M1M3M1M3 preceded and followed by sequences that contain four or five different LSAs. Thus different intervals of the record may be represented by different Markov Chains, implying a significant change in the operating dynamics of the East Asian Monsoon. The author notes that this step is interpretive, and different authors may interpret the same record differently.

Higher-order automata are generated by treating each of the generated Markov Chains as a predictive or successor state. Thus a new character string (*e.g.*,  $\mu_1\mu_4\mu_3\mu_1\mu_2$  . . .) may be characterized by one or more Markov Chains, each of which would be a third-order state, and would represent higher order structure of the dynamics of the monsoon system. The process can be repeated until only one Markov Chain remains.

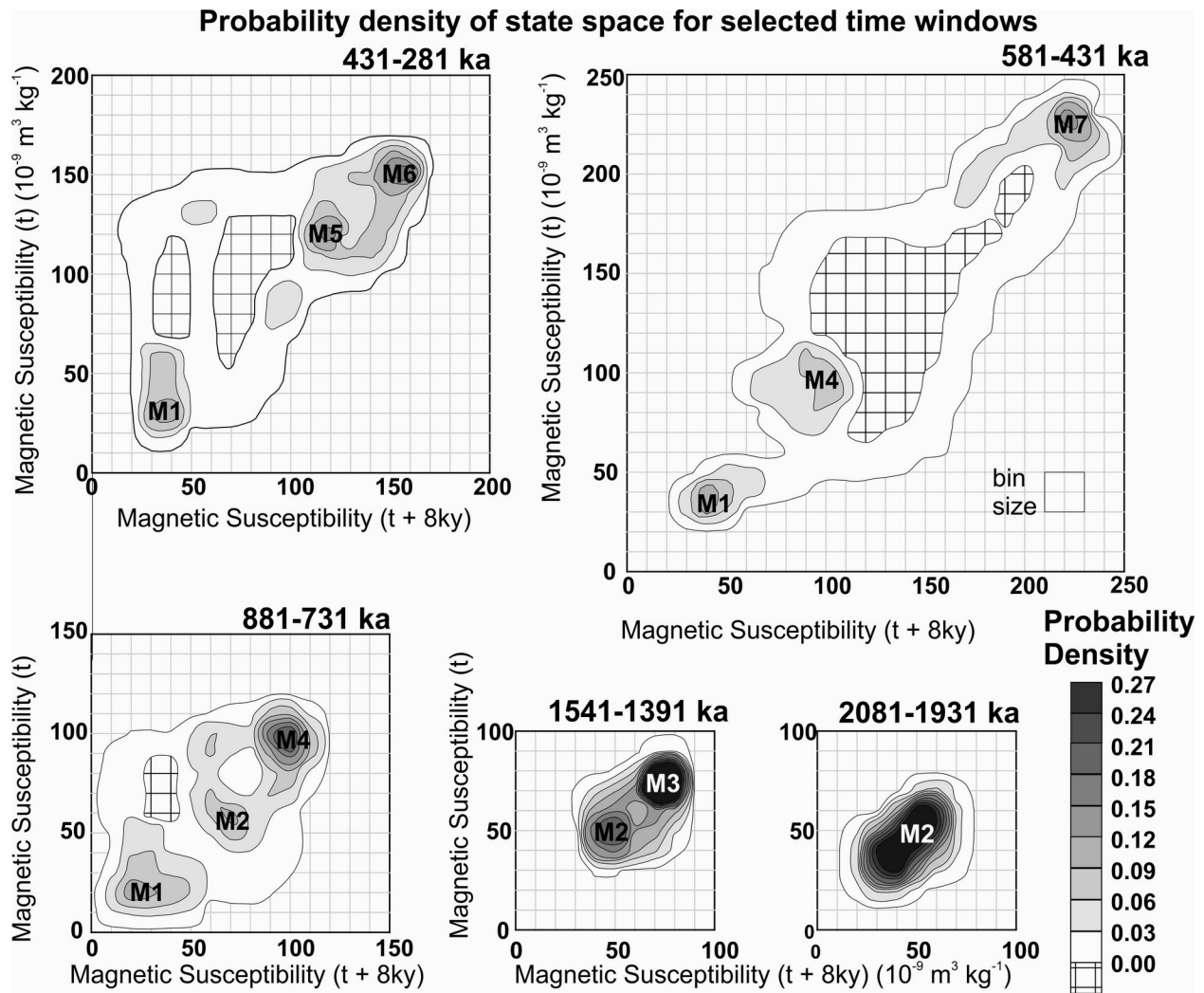
### 3 Results

#### 3.1 First-order states

The method of Gipp (2001) was used to create PDFs of reconstructed two-dimensional phase space portraits of both records. Seven regions of high probability density are observed, representing relatively stable monsoonal “states” that recur episodically throughout the Quaternary (figure 4). The number of probability density peaks that appear in any single 150-ky window over that period varies from one to five. They can be named (M1 to M7) and characterized by their location in phase space. Each region defines a first-order state, which reflects relatively stable strengths for the Himalayan monsoon on a millennial timescale.

M1 appears in the early Quaternary during the 2021-1871 ka frame, and appears intermittently until it disappears during the 1541-1271 ka frame. It appears again near during the 1391-1121 ka frame and remains until the 791-521 ka frame. M2 is the most significant probability peak in the early Quaternary (figure 4). M3 is appears in the early Quaternary until the 1751-1481 ka frame, and is not observed again until the 971-701 ka frame. M3 remains present until the 581-311 ka frame, after which it disappears. M4 appears in a few frames in the early Quaternary, around 1700 ka, and again after about 800 ka. The paleomonsoon phase space portrait expands through phase space after about 1200 ka frame, whereupon the probability peak at M5 first appears. The peak reappears late in the record after the mid-Pleistocene transition (MPT), from the 551-281 ka frame until the penultimate frame. After the MPT the phase space portrait expands to cover a much larger area of phase space. Peak M6 appears during the 641-371 ka frame and lasts until

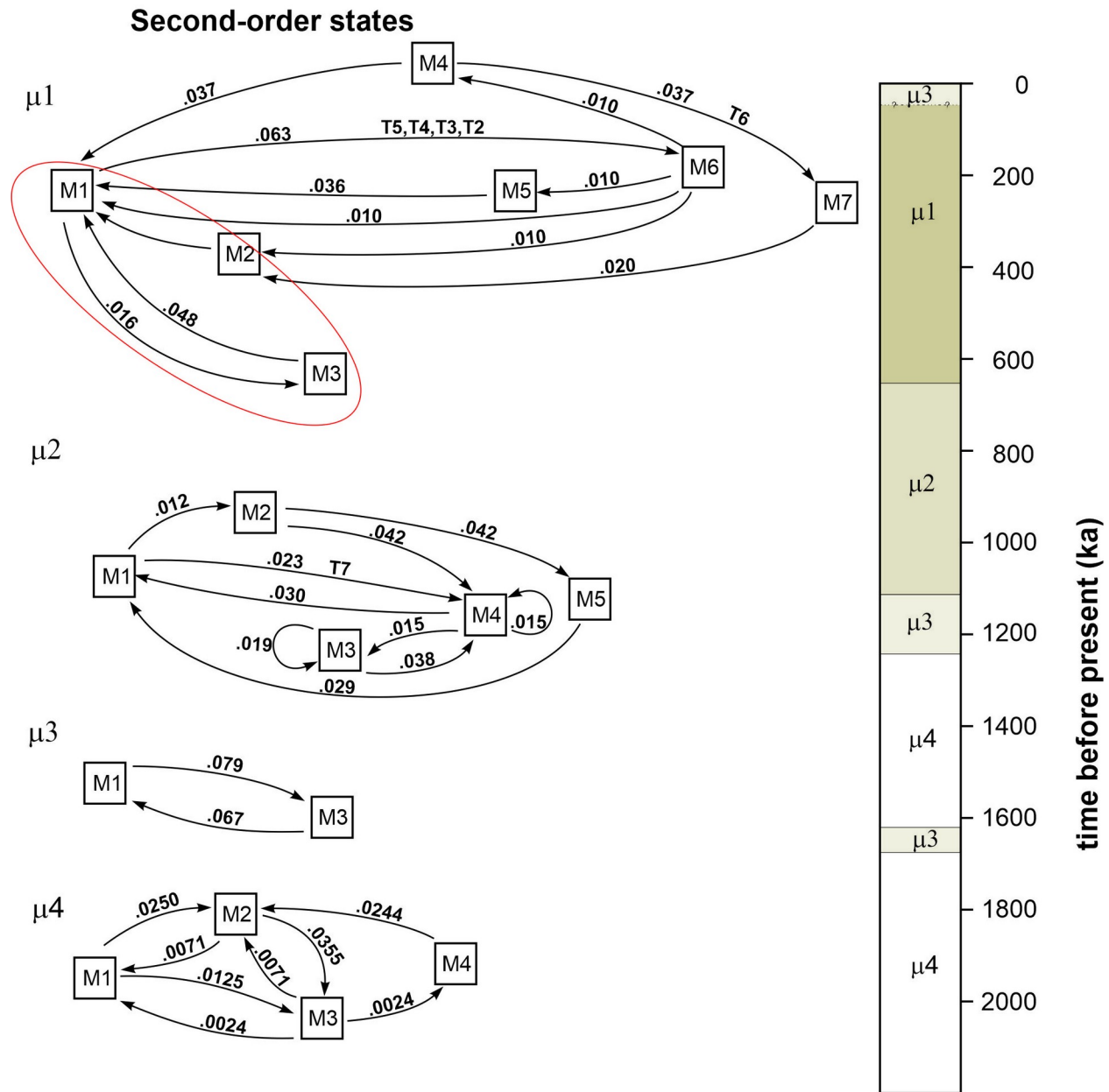
the end of the record. M7 results from a single orbit during the great excursion through phase space after the MPT (figure 4). It first appears in the 641-491 ka frame. The system only occupies M7 from 521-491 ka.



There appears to be some connection between transition in the first-order states in the East Asian Monsoon and global terminations. Major glacial terminations (T2-T7 on figure 5) occur during transitions, normally from M1 to M6 in  $\mu_1$ , and from M1 to M4 in  $\mu_2$ , suggesting that the transitions between first-order states represent global-scale shifts in dynamics, possibly driven by changes in northern hemisphere insolation.

### 3.2 Second-order states

The LSAs M1 to M7 are used as predictive and successor states in constructing a series of Markov Chains (figure 5). Four distinct Markov Chains ( $\mu_1$  to  $\mu_4$  in figure 5) have been defined from the sequence of first order states observed in the paleomonsoon record, and probabilities of transitions are calculated from the number of a particular transition (e.g., M1 to M2) divided by the total length of time that the predictive state is active. The change from one mode of behavior to another is proposed to represent a global bifurcation in the paleomonsoon system. Generally



speaking, there is an increase in complexity of behavior through the past 2.2 My, where multistability first exists between states M1, M2, M3, and M4, and as the system evolves through  $\mu_4$  to  $\mu_2$  and  $\mu_1$ , the complexity of the system increases until at least six states are required to describe it (M3 in  $\mu_1$  possibly being part of a last transition to  $\mu_3$ ). Intermittent episodes of simple oscillation between M1 and M3 punctuate this increasing complexity.

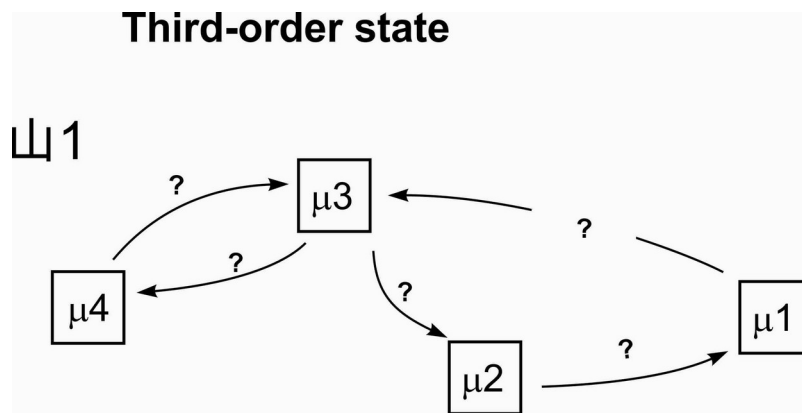
The author has not devised a completely objective method for choosing the exact boundary between, for instance,  $\mu_1$  and  $\mu_2$ . In particular, in  $\mu_1$ , there are a few transitions between M1 and M3, all of which represent the last few transitions inferred from the proxy record. Since  $\mu_3$  consists only of transitions between M1 and M3, it is possible that the proxy record may actually

indicate a transition from  $\mu_1$  to  $\mu_3$  at about 35 ka, but the author would be more comfortable waiting another 20 ky to make a definite determination.

The sequence of second-order states can be characterized by one (or possibly more) Markov chains, which may be inferred as third-order state(s). The author has not inferred the presence of more than one such state from the limited data available, but acknowledges that in a sufficiently long record, additional third-order states could be definable. If such do exist, their sequences could define higher-order states as well.

### 3.3 Third-order state

The sequence of second-order states ( $\mu_4\mu_3\mu_4\mu_3\mu_2\mu_1\mu_3$  from figure 5) can be characterized by one (or possibly more) Markov chains, which may be inferred as third-order state(s). The author has not inferred the presence of more than one such state from the limited data available, but acknowledges that in a sufficiently long record, additional third-order states could be definable. If such do exist, their sequences could define higher-order states as well. The Markov Chain from the string of second order states has been named  $\sqcup 1$  (figure 6; where  $\sqcup$ - pronounced 'shan'- is the Chinese symbol for mountain) because the timescale covered is long enough that tectonic effects have a significant chance to be the driving mechanism of the change in dynamic state. The interpretation of the transition from  $\mu_1$  to  $\mu_3$  is tentative, but if confirmed, then this state is apparently characterized by two distinct cycles—one in the Early Quaternary ( $\mu_4$  to  $\mu_3$ ) and one lasting from the MPT to the present ( $\mu_3$ – $\mu_2$ – $\mu_1$ – $\mu_3$ ).



## 4 Conclusions

The behavior of the climate system over the past two million years, as inferred from proxies for Himalayan monsoon strength, shows the characteristics of multistability. Seven observed first-order states, representing metastable states exhibit changes in sequencing suggesting ordering at a higher level. Four Markov Chains are defined, describing second order states, which could be interpreted as representing reorganizations of the climate system on a global scale. These four modes of operation partially define a higher-order state (third-order), but the record is not long enough for the third-order state to be confidently defined. Records of sufficient length may allow even higher-order states to be defined.

## Acknowledgments

The author thanks AGU for organizing the Chapman conference and the conference attendees who provided useful discussion, particularly Matt Huber and Peter Clift and also thanks two referees for reviewing this paper. The dataset for this paper appears in a supplement to Kukla *et al.* (1990).

## References

- Abarbanel, H. D. I. (1996). *Analysis of Observed Chaotic Data*. Springer-Verlag, New York.
- Abarbanel, H. D. I. & Lall, U. (1996). Nonlinear dynamics of the Great Salt Lake: system identification and prediction, *Climate Dynamics*, 12, 287-297.
- Alcocer-Cuarón, C., Rivera, A. L., & Castaño, V. M. (2014). Hierarchical structure of biological systems: A bioengineering approach. *Bioengineered* 5(2),73-79. doi: 10.4161/bioe.26570
- Anzo-Hernández, A., Gilardi-Velázquez, H. E., & Campos-Cantón, E. (2018). On multistability behavior of unstable dissipative systems. *Chaos*, 28, 033613; [doi.org/10.1063/1.5016329](https://doi.org/10.1063/1.5016329)
- Caraiani, P. (2013). Using complex networks to characterize international business cycles. *PLoS ONE* 8(3), e58109. doi: 10.1371/journal.pone.0058109
- Clift, P. D., Hodges, K. V., Heslop, D., Hannigan, R., Van Long, H., & Calves, G. (2008). Correlation of Himalayan exhumation rates and Asian monsoon intensity. *Nature Geoscience*, 1, 875-880.
- Crowley, M. F., & Epstein, I. R. (1989). Experimental and theoretical studies of a coupled chemical oscillator: phase death, multistability, and in-phase and out-of-phase entrainment. *Journal of Physical Chemistry*, 93, 2496-2502.
- Crutchfield, J. P. (1994). The calculi of emergence: Computation, dynamics, and induction. *Physica D*, 75, 11-54.
- Farnsworth, A., Lunt, D. J., Robinson, S. A., Valdes, P. J., & Robert, W. H. G. (2019). Past East Asian monsoon evolution controlled by paleogeography, not CO<sub>2</sub>. *Science Advances*, 5, eaax1697. doi: 10.1126/sciadv.aax1697
- Feudel, U. (2008). Complex dynamics in multistable systems, *International Journal of Bifurcation and Chaos*, 18, 1607, doi: 10.1142/S0218127408021233
- Feudel, U., Pisarchik, A. N., & Showalter, K. (2018). Multistability and tipping: From mathematics and physics to climate and brain—Minireview and preface to the focus issue. *Chaos*, 28, 033501, [doi.org/10.1063/1.5027718](https://doi.org/10.1063/1.5027718)
- Ghil, M., Allen, M. R., Dettinger, M. D., Ide, K., Kondrashov, D., Mann, M. E. *et al.* (2002), Advanced spectral methods for climatic time series. *Reviews of Geophysics*, 40, 3-1—3-41. doi: 10.1029/2000RG000092
- Gipp, M. R. (2001). Interpretation of climate dynamics from phase space portraits: Is the climate system strange or just different? *Paleoceanography*, 16, 335-351.
- Guimerà, R., Danon, L., Diaz-Guilera, A., Giralt, F., & Arenas, A. (2003). Self-similar community structure in a network of human interactions. *Physical Review E*, 76, 046118.
- Han, M., Ren, W., Xu, M., & Qiu, T. (2019). Nonuniform State Space Reconstruction for Multivariate Chaotic Time Series. *IEEE Transactions on Cybernetics*, 49(5), 1885-1895, doi: 10.1109/TCYB.2018.2816657.
- Hirsch, M. W. & Smale, S. (1974), *Differential Equations, Dynamical Systems and Linear Algebra*, Academic, San Diego, Calif.
- Kauffman, S. (1993). *The Origins of Order: Self-Organization and Selection in Evolution*, Oxford Univ. Press, New York, 734 p.
- Kelso, J. A. S. (2012). Multistability and metastability: understanding dynamic coordination in the brain. *Transactions of the Royal Society B: Biological Sciences*, 367:906-918.

- Kleidon, A. (2012). How does the Earth system generate and maintain thermodynamic disequilibrium and what does it imply for the future of the planet? *Transactions of the Royal Society A.*, 370, 1012-1040. doi: 10.1098/rsta.2011.0316.
- Kukla, G., An, Z. S., Melice, J. L., Gavin, J., & Xiao, J. L. (1990). Magnetic susceptibility record of Chinese loess. *Royal Society of Edinburgh: Earth Sciences.*, 81: 263-288.
- Liu, Q., Weerman, E. J., Gupta, R., Herman, P. M. J., Olff, H., & Koppel, J. (2014). Biogenic gradients in algal density affect the emergent properties of spatially self-organized mussel beds. *Journal of the Royal Society Interface*, 11(96), 20140089.
- Lorenz, E. N., 1963. Deterministic nonperiodic flow. *Journal of the Atmospheric Sciences*, 20, 130-141.
- Lucarini, V. & Bódai, T. (2016). Melancholia states in the climate system: Exploring global instabilities and critical transitions. *Nonlinearity*, 30(7), doi: 10.1018/1361-6544/aa6b11.
- Lyapunov, A. M. (1966), *Stability of Motion*, Academic Press, New York.
- Menzies, C. D., Wright, S. L., Craw, D., James, R. H., Alt, J. C., Cox, S. C, Pitcairn, I. K., &Teagle, D. A. H. (2018). Carbon dioxide generation and drawdown during active orogenesis of siliciclastic rocks in the Southern Alps, New Zealand. *Earth and Planetary Science Letters*, 481, 305-315. doi.org/10.1016/j.epsl.2017.10.010.
- Merrill, S. (2010). Markov chains for identifying nonlinear dynamics. In S. J. Guastello and A. Gregson (eds.), *Nonlinear dynamical systems analysis for the behavioral sciences using real data*. CRC Press, New York, pp. 401-423.
- Mihm, J., Loch, C. H., Wilkinson, D. H., & Huberman, B. A. (2010), Hierarchical structure and search in complex organizations. *Management Science*, 56, 831-848.
- Nicolis, G. (1987). Bifurcation and stochastic analysis of nonlinear systems: An introduction. In G. Nicolis (ed.), *Irreversible Phenomena and Dynamical Systems Analysis in Geosciences*. NATO Science Series C. Springer Netherlands, pp. 3-29.
- Okasha, S. (2012). Emergence, hierarchy and top-down causation in evolutionary biology. *Interface Focus*, 2: 49-54. doi: 10.1098/rsfs.2011.0046.
- Packard, N. H., Crutchfield, J. P., Farmer, J. D., & Shaw, R. S. (1980). Geometry from a time series, *Physical Review Letters*, 45: 712-716.
- Paillard, D. (2001). Glacial cycles: Toward a new paradigm. *Reviews of Geophysics*, 3, 325-346.
- Pattee, H. H. (1972). The nature of hierarchical controls in living matter. In R. Rosen (ed.), *Foundations of Mathematical Biology*. Academic Press, New York, pp. 1-22.
- Robinson, A., Calov, R., & Ganopolski, A. (2012). Multistability and critical thresholds of the Greenland ice sheet. *Nature Climate Change*, 2, 429-432.
- Spicer, R., Yang, J., Herman, A, Kodrul, T., Alksandrova, G., Maslova, N., et al. (2017). Paleogene monsoons across India and South China: Drivers of biotic change. *Gondwana Research*, 49, 350-363. doi.org/10.1016/j.gr.2017.06.006
- Strelioff, C. C., Crutchfield, J. P., & Hubler, A. (2007). Inferring Markov Chains: Bayesian Estimation, Model Comparison, Entropy Rate, and Out-of-class Modeling, *Physical Review E*, 76,011106.
- Sun, X. & Wang, P. (2005). How old is the Asian monsoon system?—Palaeobotanical records from China. *Palaeogeography, Palaeoclimatology, Palaeoecology*, 222, 181-222.

**Figure 1.** Reconstructing phase space from data sets. a) Phase space created in three dimensions from three data sets ( $\omega$ ,  $\Phi$ ,  $\Gamma$ ). b) The time delay method of Packard *et al.* (1980) is used to convert the time series  $\Phi(t)$  at left into a two-dimensional phase space (right).

**Figure 2.** Possible behaviours in reconstructed phase space portraits. a) Sequence of disjoint regions of stability of different types, including limit cycle, Lyapunov stability, and asymptotic stability (point attractors). b) Chaotic “strange attractor” (after Lorenz, 1963).

**Figure 3.** Trajectory of the reconstructed phase space of the East Asian monsoon showing the relationship between LSAs identified from probability density. Stability is represented by the trajectory remaining in relatively small regions of phase space for extended periods of time. Filled circles represent 10 ky intervals. Note the contrast between the distance travelled in one 10 ky interval during times of stability vs. during times of transition.

**Figure 4.** Probability density plots of the reconstructed state space of the Himalayan paleomonsoon over five selected timeframes. In the early Quaternary (lower three frames) there were three stable monsoonal strengths (first-order states): M1, which is comparable to the Himalayan monsoonal strength during the last glacial maximum, M2, and M3. The Mid-Pleistocene transition (lower left and above) there is a rapid expansion of the function into previously inaccessible areas of phase space.

**Figure 5.** Second-order states for the Himalayan paleomonsoon strength proxy. T7, T6, *etc.*, represent Late Quaternary glacial terminations. Red ellipse covers the last few transitions and may signify a return to state  $\mu_3$ . Further explanation in text.

**Figure 6.** Construction of proposed third-order state for the Himalayan paleomonsoon, using the Chinese character for “mountain” (pronounced ‘shan’). The third-order state cannot be completely defined by the data at hand—a longer record is required. There are not enough observed transitions between second-order states to be confident in estimated probabilities. Also, there is not enough certainty from the most recent part of the record to establish whether the system has recently made the transition to  $\mu_3$ , or whether the recent behaviour is a part of  $\mu_1$ . The overall structure is suggestive of two types of cyclic behaviors – the first between  $\mu_4$  and  $\mu_3$  in the Early Quaternary, the second a cycle through  $\mu_2$  and  $\mu_1$  from the mid-to-late Quaternary.